

**COMPUTER AIDED TISSUE ENGINEERING FOR THE  
GENERATION OF UNIT LIBRARY STRUCTURE OF  
SCAFFOLD FOR HUMAN BONE (*in-vitro*)**

*A Thesis submitted in partial fulfilment of the requirements for the degree of*

*Master of Technology*

*in*

*Biomedical Engineering*

*by*

**ROHAN VINAYAK BHAGWAT**

**213BM1002**

Under The Supervision of

**Prof. (Mrs.) Krishna Pramanik**



**Department of Biotechnology & Medical Engineering  
National Institute of Technology  
Rourkela-769008, Orissa, India  
June, 2015**



**National Institute of Technology  
Rourkela**

**CERTIFICATE**

This is to certify that the thesis entitled, “**COMPUTER AIDED TISSUE ENGINEERING FOR THE GENERATION OF UNIT LIBRARY STRUCTURE OF SCAFFOLD FOR HUMAN BONE (in-vitro)**” submitted by **Rohan Vinayak Bhagwat (213BM1002)** in partial fulfillment of the requirements for the award of degree of **Master of Technology in Biomedical Engineering** at National Institute of Technology, Rourkela is an authentic work carried out by him under my supervision and guidance. To the best of my knowledge, the matter embodied in the thesis has not been submitted to any other University/Institute for the award of any Degree or Diploma.

Place: Rourkela

Date

Supervisor

**Prof. Krishna Pramanik**

Department of Biotechnology and Medical Engineering

National Institute of Technology, Rourkela-769008

## **DECLARATION**

The present study entitled “**COMPUTER AIDED TISSUE ENGINEERING FOR THE GENERATION OF UNIT LIBRARY STRUCTURE OF SCAFFOLD FOR HUMAN BONE (in-vitro)**” is based on my original research work and no part of the thesis has been so far submitted for the award of degree in Master of Technology in Biomedical engineering or any other degree or diploma to the NIT Rourkela, Orissa, India or elsewhere.

**Place: Rourkela, Odhisa**

**ROHAN VINAYAK BHAGWAT**

**Date:**

## ACKNOWLEDGEMENT

*It is my pleasure to take the opportunity of expressing my sincere gratitude to all those people who provided their support, collaboration and encouragement to carry out my dissertation work. This project helped me a lot to extract out practical knowledge from theoretical work.*

*First of all I would like to thank my supervisor, **Prof. Krishna Pramanik**, HOD, Department of Biotechnology and Medical Engineering, NIT Rourkela, for her invaluable guidance and help in my dissertation work. I also thank her for guiding me during every part of my work, for helping me improve upon my mistakes all through the project work and for her kind cooperation, motivation and providing experimental expertise required in my work.*

*I would like to extend my thanks to **Dr. Sunil K. Sarangi**, Director, National Institute of Technology, Rourkela for providing the opportunity and facilities to pursue this work at the institute.*

*I have an overwhelming sense of gratitude to Dr. Niladri Panda, Mr. Partha Sarthi Majhi, Mr. Chitranjan Bhoi, Mr. Basil Mathai, Mr. Sheeshan Jena, Mr. Punit Ahalawat and Mr. Deepradyuti Sen for imparting knowledge on various topics of my field of research and actively concerned about experimental analysis. I have learnt many experimental techniques from them. I appreciate the skills and art they have, to make others understand any problem. I am also thankful to entire technical and non-teaching staff of Department of Biotechnology and Medical Engineering, NIT Rourkela for their co-operation and help in completing my dissertation work.*

*I would like to thank my colleagues Amit, Anurag, Trupti, Varshini mam, Sahely mam and friends Ram, Dinesh, Sumran, Iqbal, Nilesh, Hitesh, Chetan, Kiran, Abhishek, Aasis and Mayuri for always being supportive to me.*

*Finally, I would like to express my sincere gratitude to my parents Mr. Vinayak Bhagwat and Mrs. Ratna Bhagwat. I am extremely grateful to my Uncle Mr. Parag Moon, my sister Pooja Bhagwat and brother Vishesh Bhagwat for believing, inspiring and supporting me at every step of my life.*

**Rohan Vinayak Bhagwat**

# CONTENTS

<b>Certificate</b>	i
<b>Acknowledgement</b>	iii
<b>List of Figures</b>	v
<b>List of Tables</b>	vi
<b>Nomenclature</b>	vii
<b>Abbreviations</b>	viii
<b>Abstract</b>	ix

<b>Chapter</b>	<b>Title</b>	<b>Page</b>
<b>No</b>		<b>No</b>
<b>1</b>	<b>Introduction and objective</b>	<b>1</b>
<b>2</b>	<b>Literature Review</b>	<b>5</b>
<b>3</b>	<b>Methodology</b>	<b>10</b>
	3.1 Image Acquisition	11
	3.2 3D Reconstruction from 2D scans	13
	3.3 Designing of unit library structure of scaffold	17
	3.4 Designs made in Solidworks	21
	3.5 FEA in ANSYS Workbench	24
	3.6 Shaping the bulk scaffold	28
	3.7 Fused Deposition Modelling	30
<b>4</b>	<b>Result and Discussions</b>	<b>31</b>
	4.1 Porosity of designs	32
	4.2 Effective modulus of designs	33
	4.3 Intersection Index	37
	4.4 Equivalent Von-Mises stress distribution in designs	38
<b>5</b>	<b>Conclusion</b>	<b>40</b>
	<b>Future Prospects</b>	<b>42</b>
	<b>References</b>	<b>44</b>

## LIST OF FIGURES

<b>Figure No</b>	<b>Name</b>	<b>Page No</b>
1	Flow chart of Computer Aided Tissue Engineering	3
2	Working of CT scan machine	12
3	Working of MRI machine	13
4	Micro DICOM software GUI	14
5	Selection of ROI in In-Vesalius	15
6	Selection of threshold in In-Vesalius	15
7	3D Reconstruction in In-Vesalius	16
8	Final 3D reconstructed foot	17
9	Isolated bone from 3D model using Geomagics	17
10	Enclosed pores during designing	19
11	Designs D1,D2,D3,D4,D5 in Solidworks	22
12	Designs D6,D7,D8,D9,D10 in Solidworks	23
13	Meshing in ANSYS	25
14	Displacement and supports in (i) Confined case and(ii) Unconfined case	26
15	Displacement in Design for calculating effective modulus	27
16	Images showing cross-sectional planar images of 3D bone	28
17	Recreated bone in Solidworks	29
18	Bulk structure of D3 unit library design	30
19	Final model for printing	30
20	Equivalent Von Mises stress in designs D2, D3, D7 and D8	39

## LIST OF TABLES

<b>Table No</b>	<b>Name</b>	<b>Page No</b>
1	Materials and their mechanical properties for using in ANSYS	25
2	Results showing porosity of unit scaffold structure	32
3	Reaction force and cross-sectional area for different designs and materials in confined conditions	33
4	Effective modulus of designs for different designs and materials in confined conditions	34
5	Reaction force and cross-sectional area for different designs and materials in unconfined conditions	35
6	Effective modulus of designs for different designs and materials in unconfined conditions	36
7	Intersection Index for all designs	37
8	Equivalent Von Mises Stress distribution in all designs	38

## NOMENCLATURE

Symbol	Definition
$\emptyset$	Porosity
$F_1$	Face 1
$L_0$	Original length
$L_1$	Change in length
$\epsilon$	Strain
$\sigma$	Stress
$E_{\text{effective}}$	Total effective modulus
$E_x, E_y, E_z$	Effective modulus in x, y, z direction respectively
$R_y$	Reaction force in y direction
$A_y$	Cross-sectional area on face 1



## ABBREVIATIONS

Name	Full form
CATE	Computer Aided Tissue Engineering
2D	Two Dimensional
3D	Three Dimensional
FEA	Finite Element Analysis
II	Intersection Index
CT	Computed Tomography
MRI	Magnetic Resonance Imaging
CAD	Computer Aided Designing
CAM	Computer Aided Manufacturing
ROI	Region of Interest
STL	Standard Tessellation Language
Mat A	Material A
GPa	Giga Pascal
MPa	Mega Pascal
N	Newton
PLLA	Poly Lactic acid
PLGA	Poly co glycol lactic acid

## **ABSTRACT**

Tissue engineering scaffold is a biological substitute that aims to restore, maintain or to improve tissue functions. The scaffold for orthopedic surgeries need to be designed very accurately for absolute benefit to the patient. In this study various unit library structure designs for scaffold are presented for improvement in scaffold characteristics and advancements in its applications. These structures are designed to achieve the specific mechanical structure and properties which are superior to the available conventional techniques of scaffold fabrication. As the requirements for a better scaffold are met adequately through better and appropriate designing techniques, the prospects of fabricating a more successful engineering scaffold also improves. In this study, Finite element analysis was performed to investigate the characteristic features of the unit library structure designs to evaluate and examine their mechanical properties including porosity, effective modulus, compatibility with other designs and stress distribution. DICOM images for human foot were processed and reconstructed using image processing tools and 3D reconstruction software. The validated design of unit library structure was made in the bulk form and given a shape of reconstructed bone. Fused Deposition Modelling was used to manufacture the validated design.

### **Keywords**

Orthopedic Tissue engineering, scaffold, unit structure, porosity, stress distribution, Computer aided design, DICOM, fused deposition modelling

**CHAPTER 1**

***INTRODUCTION AND OBJECTIVES***

# INTRODUCTION

## **1.1 Tissue Engineering:**

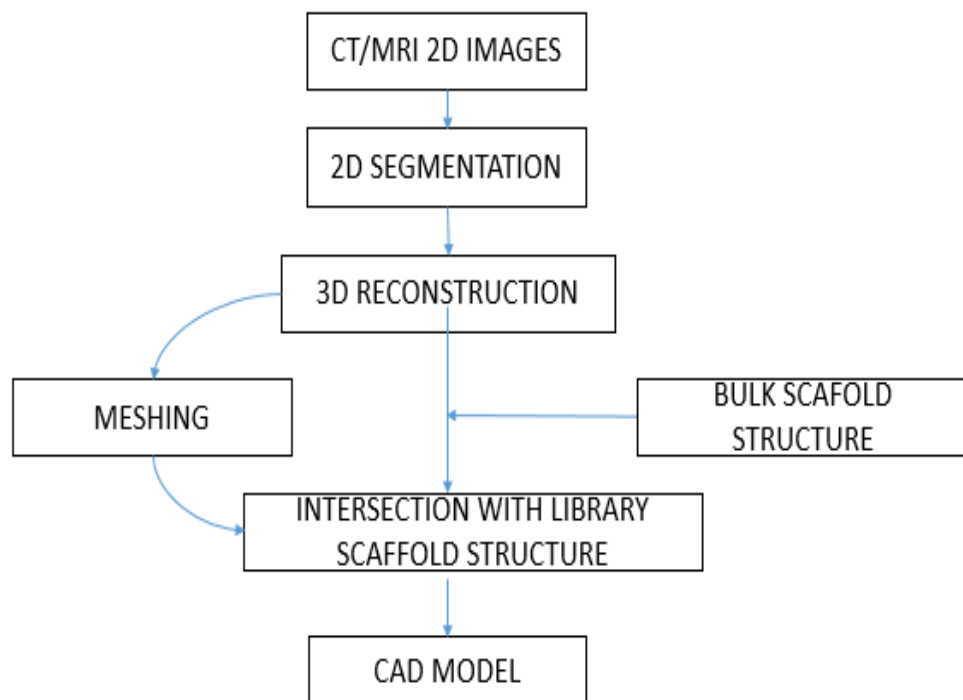
The combination of cellular engineering, material methods as well as suitable biological and physiological factors for the improvement biological functions and to replicate or mimic the biological functions or to replace them is termed as Tissue Engineering (TE). Most of the definitions of TE covers a vast range of applications, practically the term applies to restore or substitute the tissues in living body. The tissues involved require specific structural and mechanical properties. It also refers performing the biochemical functions using cells within artificially mimicked environment; for example artificial liver. It is also used often along with regenerative medicine and use of stem cells and progenitor cells to grow new tissues. Scaffolds are the mechanical support or the framework on which the cell culture takes place. It provides the basic environment to the formation of new tissue. Thus design of scaffold plays a very important role in Tissue Engineering.

## **1.2 Need of Computer aided Designing:**

Computer Aided Tissue Engineering (CATE) ; It is the revolution in the field of biology and bioengineering and has created a platform in which the advancements in the life sciences are not only responsive but they also need active involvement of engineering design and development. Successful scaffold should possess three properties; sufficient cell adhesion, adequate fluid perfusion and the required mechanical strength which provides it the support during healing and degradation. First two properties are achieved in scaffolds fabricated by conventional techniques of but the third property i.e. mechanical strength is not satisfactory due to indiscretions in the formation of scaffold. About 60 % porous scaffold provides adequate cell adhesion and fluid perfusion. In cases of high load bearing implants like treatment of spine and long bones, the

conventional techniques might fail. If a scaffold with insufficient mechanical strength is used then it may allow tissue invasion and fluid perfusion but as a result of this the failure of design could be the consequence. The random architecture obtained in conventional methods is responsible for low mechanical integrity and the enlarged pore size to allow fluid perfusion can also be considered as a degrading factor in mechanical strength. To achieve the sufficient mechanical strength, advanced designing and manufacturing is essential. In this context we can use advanced techniques like rapid prototyping to fabricate the scaffolds with improved properties, further FEA (Finite element analysis) helps for virtual simulations and estimates the nearly equivalent properties possessed by the structure prior to its real manufacturing.

**1.3 Flow Chart of CATE:** Fig.1 depicts the flow chart of computer aided tissue engineering



*Figure 1: Flow chart of Computer aided Tissue Engineering*

## **OBJECTIVES**

The specific objective of this thesis work is as follows:

- Acquisition of 2D DICOM scans and 3D reconstruction
- Design of unit structures in Solidworks
- FEA in ANSYS Workbench
- Creation of a demonstration model using Rapid Prototyping technique

**CHAPTER 2**

***LITERATURE REVIEW***

Wei Sun *et al* discussed the application of computer aided designing approach for biomimetic scaffold. A deep study of image acquisition and reconstruction of 3D model is presented. Quantitative CT (Computed Tomography) characterization, FEA (Finite Element Analysis) and freeform extruding deposition for scaffold making is described. The method to analyze the effective modulus of the design is given in the paper.[1]

Bucklen *et al* presented tissue primitive libraries and interfaces which can be implemented in CATE (Computer aided tissue engineering). They discussed about many biomaterials lack in properties same as bone and hence the possibilities of design mimicking the bone is focused. Due to unavailability of suitable biomaterials, the designing of the scaffold becomes very important because it provides the basic requirements for TE i.e. cell adhesion, perfusion and growth.[2]

Shengyong Cai *et al* emphasized the meshing techniques of the unit library structures. A method was proposed in which the subject was divided into several quadrilaterals depending on their densities and then using mathematical equations spheres were created in each quadrilateral and then meshing structure was formed.[3]

Nattapon *et al* suggested the criteria to design a scaffold. Three criterias were suggested regarding the making of unit structure viz. **Criteria A**: The feasibility of the manufacturing machine should be kept in mind, **Criteria B**: the designs should be combined with itself or other design units as necessary and **Criteria C**: Enclosed pores should not be present in between the unit blocks as this decreased the porosity of the structures. Also the formula to determine the porosity of unit volume structure is mentioned.[4]

Wettergreen *et al* demonstrated the creation of unit library of architectures for scaffold fabrication that can be used to make complex scaffolds. It became easier to design a small unit and focus on



its mechanical properties and design, further the whole model can be formed with required properties. Method to compare various designs using Finite Element Analysis was described and the stress distribution over entire unit block was shown for each and every design.[5]

Kentaro Iwami *et al* emphasized the use of rapid prototyping over other techniques due to the development scope in design of RP machines and the broadened range of materials from hard and dry to soft and wet. In the study a rapid prototyping system was designed based on extrusion model and relation between speed of movement of nozzle head and pressure applied were studied during the formation of lines of scaffold.[6]

Shelby A. Skoog *et al* in their study suggested that stereolithography can be used to make a scaffold which is specific to a particular patient. Photo-polymerization based techniques for rapid prototyping which are optimized techniques also called as two photon polymerization may be used to create TE scaffolds with small feature size along with high resolution and precise dimensions as compared to conventional stereolithography techniques.[7]

Hutmatcher *et al* in their study have done many studies practical and theoretical and concluded that there is no such biomaterial yet developed which can be an exact copy of human bone in properties.[8]

Susmita Bose *et al* in their study described the necessity of developing a good scaffold for implant making because body cannot itself heal major injuries. As a future development it was suggested that among all the additive manufacturing techniques, 3D printing is the most promising technique to manufacture scaffold. Also 3D printed scaffolds are used for drug delivery.[9]

Giannitelli *et al* used various mathematical expressions to create new designs that can be used in the manufacturing process of the scaffold. These designs expressed uniformity throughout the bulk model. Also the advantages of hydrogels as a biomaterial for scaffold making are discussed.[10]

Podshivalov *et al* have shown a new approach for the design of micro scale scaffold from the biocompatible composites. FEA was done considering the Young's modulus of trabecular bone 2GPa and Poisson's ratio 0.3. Results were obtained in form of Von Mises stress distribution in scaffold.[11]

Weinand *et al* used hydrogel beta TCP scaffolds in his experiments to make scaffolds and deeply studied the behavior of mesenchymal stem cells over them for a prolonged duration. He also suggested use of hydrogels along with the biomaterial used to make 3D printed scaffold to achieve specific mechanical strength and porosity along with cell adhesion and proliferation.[12]

Leong *et al* compared different polymer scaffold processing techniques for scaffold manufacturing like fiber bonding, phase separation, solvent casting and particulate leaching, membrane lamination, melt moulding, freeze drying and described their pros and cons. moreover it was concluded that solid free form fabrication (SFF) or 3D printing which includes Selective layer sintering and Fused deposition modelling are superior over other techniques.[13]

Azrulhizam *et al* have shown in their paper a new concept to convert DICOM images in other format which can be used to construct 3D images from 2D images. Thus CAD can be associated with DICOM to form 3D reconstructed objects.[14]

Quadrani *et al* made a scaffold from porous ceramic bulk which was a 3D prototype with micro and macro porosity and interconnectivity between the pores. In this study mimicking the properties of human spongy bone was tried.[15]

Landers *et al* used a new technique of 3D printing i.e. dispensing technique which was developed in year 2000. Using this a soft tissue scaffold of nose was made. The new thing about this process was that the placement of dispensing process in the bath of liquid with matched density. This allowed a wide range of materials to be used including melts, pastes, resins and hydrogel. This technique eliminated the need of extra support structure.[16]

Masood *et al* described the use of polyhedral shapes of open structures can effectively be used as basic unit block for making scaffold.[17]

**CHAPTER 3**

***METHODOLOGY***

### **3.1 IMAGE ACQUISITION**

In order to construct or design a scaffold, its shape and structure must be analyzed and observed. These can be done by image acquisition. Various imaging modalities are available for the acquisition of images.

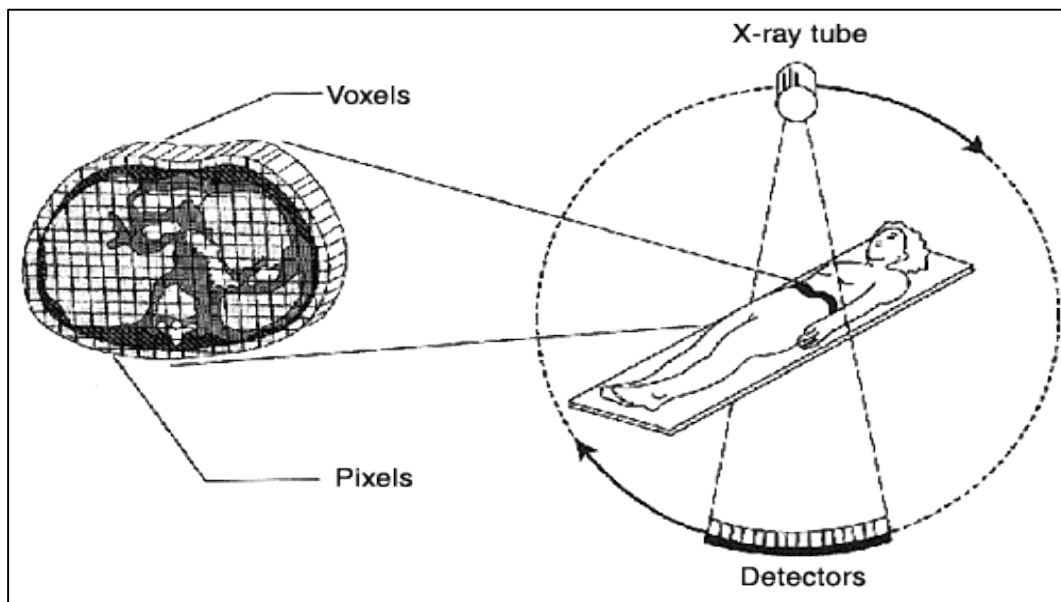
Few modalities are listed as:

- X-rays
- Ultrasound
- Computed Tomography scan
- Magnetic Resonance Imaging
- PET-CT (Positron Emission Tomography-Computed Tomography)
- SPECT (Single Photon Emission Computed Tomography)

#### **3.1.1 CT SCAN**

CT (Computed Tomography) also known as CAT (Computer Aided Tomography) is a medical imaging method which uses X-rays as a source to generate the images of internal body organs. It comprises of usage of multiple X-ray sources and multiple detectors, all these assembly is designed in such a way that we can take multiple projections from different angles for producing a detailed cross-sectional image of organs within the body. The working of CT scan is shown in Fig.2. This is noninvasive imaging modality and does not require any special operation on patient, imaging is done without any cut on a patient's body. CT images allows the doctors to get a very precise three dimensional (3D) views of the internal structure of human body including soft tissues, bones and organs such as lungs, pelvis, heart, abdomen, blood vessels.

CT provides very clear imaging of the bones. As the bones are opaque and high in density than other tissues, they absorb large amount of X-rays. When CT is used for imaging of bones, very clear and specific images of interest are obtained. A particular deformed bone can be targeted and a clear three dimensional (3D) imaging of the deformation using CT.



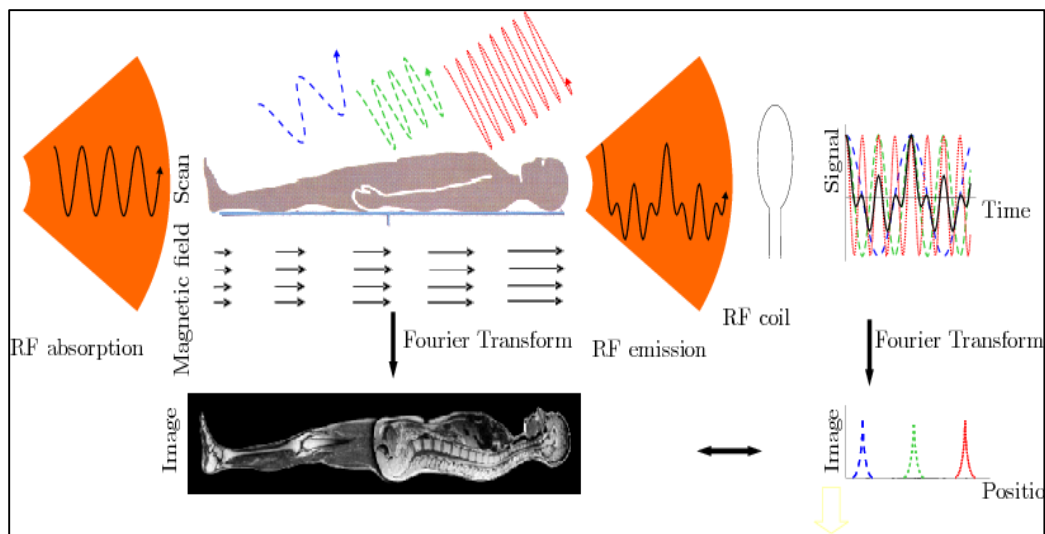
*Figure 2: Working of CT scan machine [18]*

### **3.1.2 MRI**

MRI (Magnetic Resonance Imaging) is an another medical imaging method which uses magnetic fields and radio waves to create detailed images of the soft tissues and organs within the human body. MRI is also a noninvasive method and does not require any operations on patient prior to imaging tests. MRI has been proved very effective in diagnosis of a number of conditions by presenting difference between normal tissues and diseased tissues of body. The working of MRI is shown in Fig.3

MRI is often used to evaluate blood vessels, abnormal tissues, joints in bones, brain, various organs (heart, kidney, liver etc.) also tendon injuries and ligament tear.

This modality can be used for precise and accurate 3D imaging of tissues. Thus assisting in designing of shape for scaffold for tissues.



*Figure 3 Working of MRI Machine [19]*

### **3.1.3 Universal format for medical imaging:**

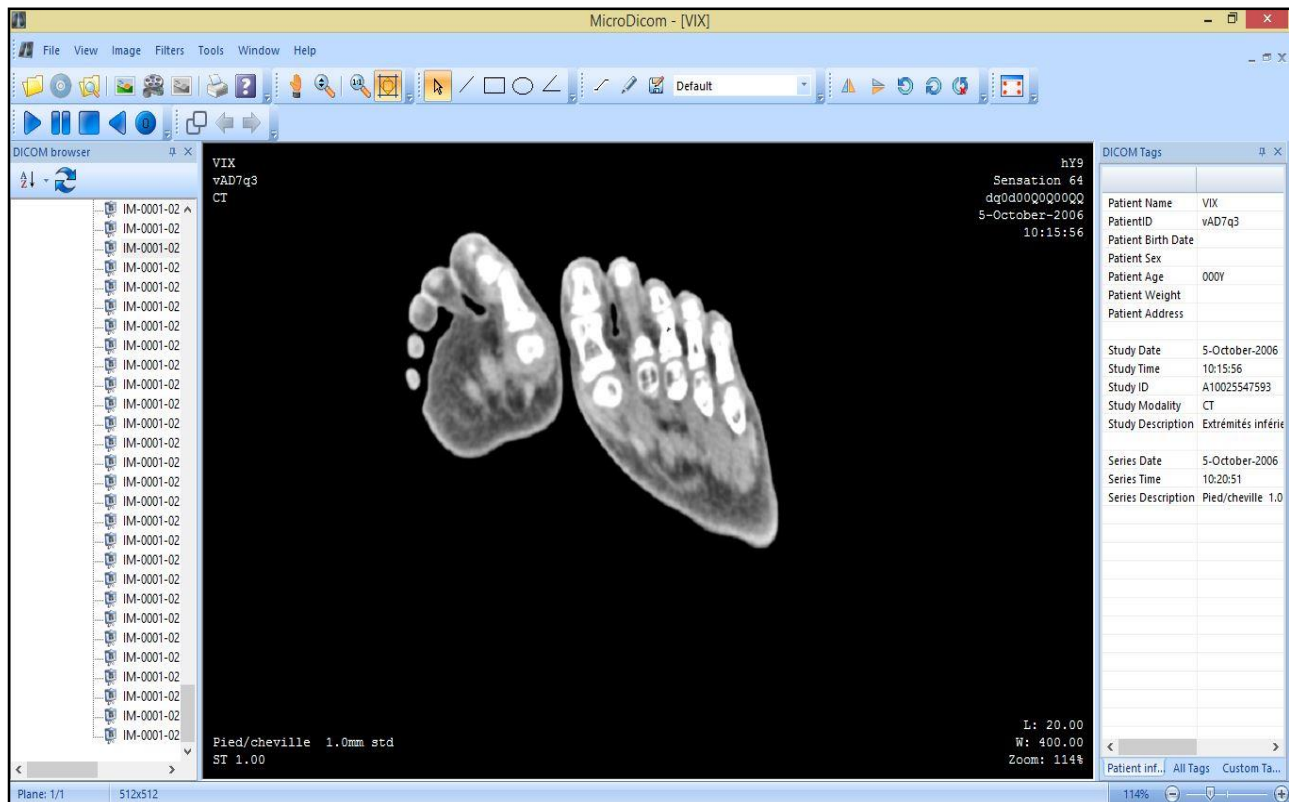
Digital Imaging and Communications in Medicine (DICOM) is the format used for storing, operating and transmitting the images scanned from the various invasive and noninvasive medical modalities. These images are then analyzed, processed and reconstructed to form the 3D model which gives an exact idea of the required shape of scaffold design.

### **3.2 3D RECONSTRUCTION FROM 2D CT SCANS**

In this study CT scans for human leg are acquired from the website <http://www.osirix-viewer.com/datasets/> [22]

### 3.2.1 Micro DICOM viewer

Micro DICOM is an application for preliminary processing of the medical images in DICOM format. This software is a freeware, accessible to all. The user interface of software is shown in Fig.4. It is used to view the DICOM images and also browse the DICOM directories. [20]



*Figure 4: Micro DICOM Software GUI*

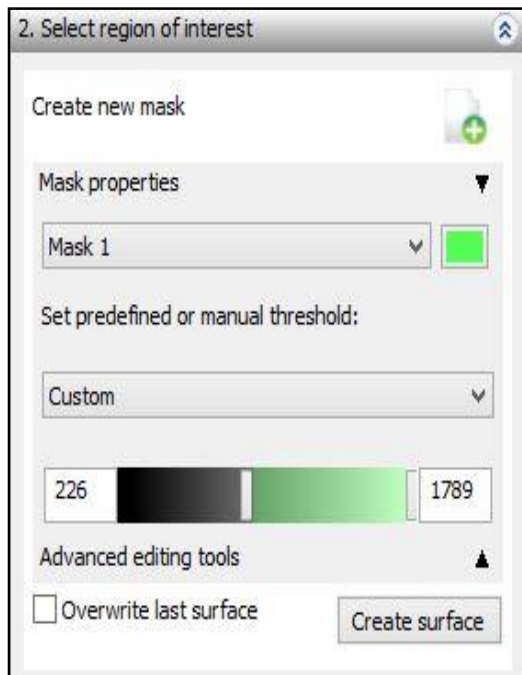
### 3.2.2 In-Vesalius 3.0

This software is a freeware and is used to generate 3D medical imaging reconstruction based on a sequence of 2D DICOM files acquired with CT or MRI imaging modalities. The required properties from the scans can be selected and then they can be given as input for 3D reconstruction. [21]

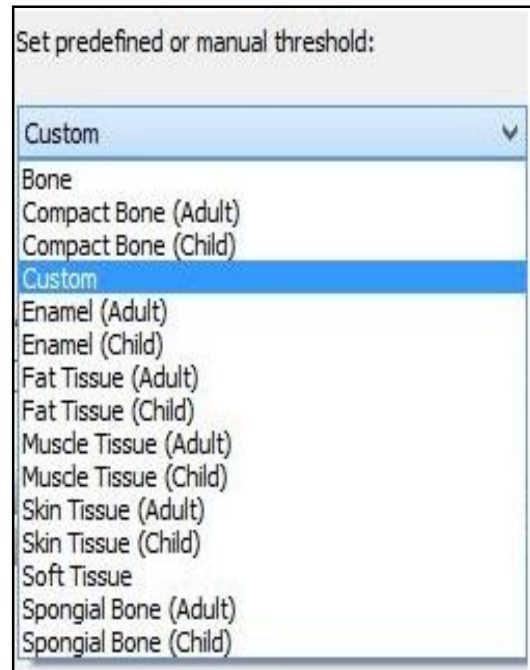


## Procedure to create a 3D model:

The software is started and then to load images, select File>Import DICOM> Browse for folder > Select the folder with DICOM images. Imported data is displayed on the screen. The import option in lower left is used to select slides to import. Then resolution reduction percentage is selected, this depends on the available memory of the system. The next section is to select Region of interest (ROI) i.e. a threshold should be specified which can be considered in the 3D model respectively shown in Fig.5 and Fig6

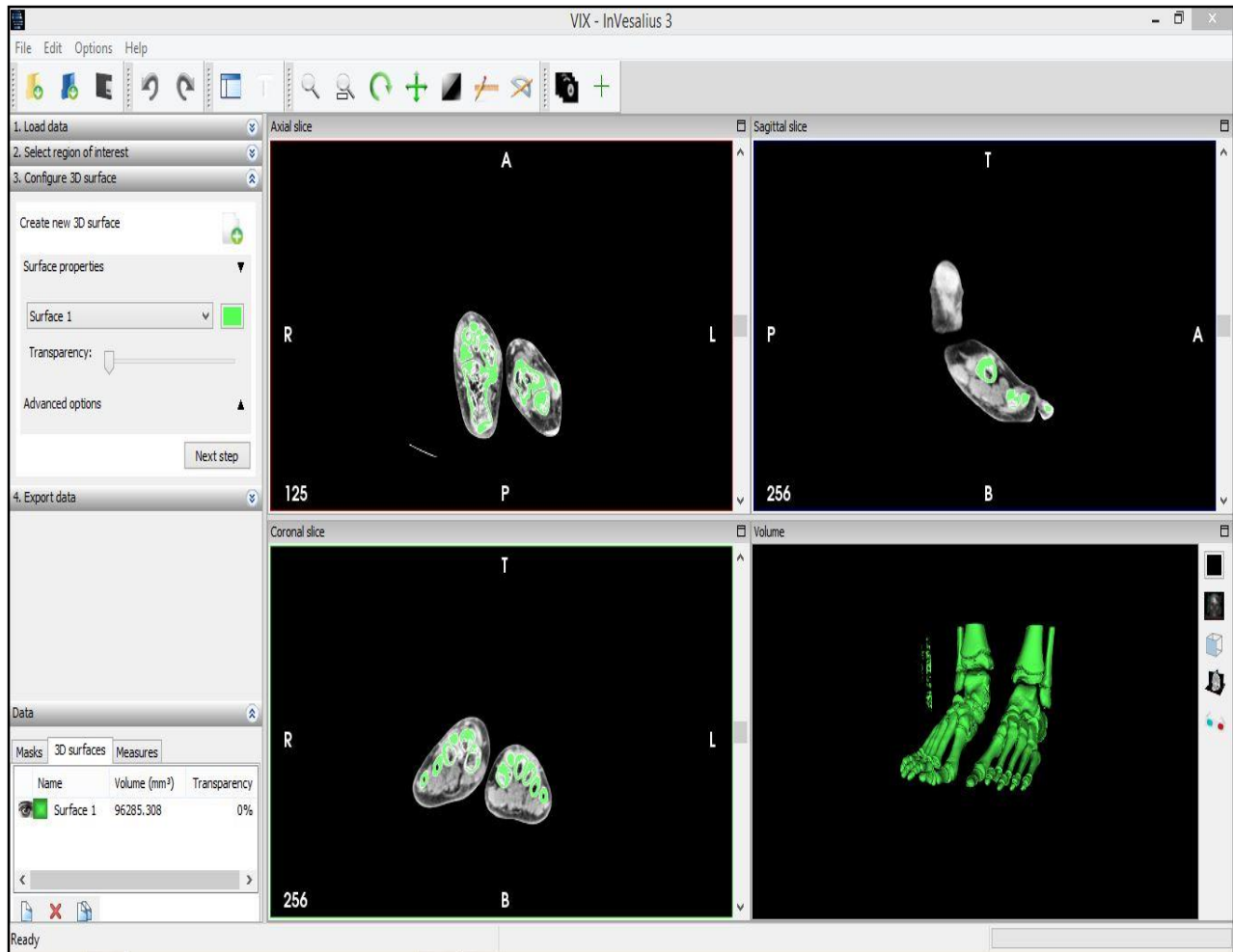


*Figure 5: Selection of region of interest in In-Vesalius*



*Figure 6: Selection of threshold in In-Vesalius*

Different masking is set depending on the number of features that are needed to be included in the 3D reconstruction and predefined manual threshold is used to select the bone, tissue etc. from scans. Bone is selected and surface is created. Data is exported in the required format to save the 3D model. 3D reconstruction interface is shown in Fig.7



*Figure 7: 3D reconstruction in In-Vesalius*

Standard Tessellation Language (STL) or Stereo-lithography format is widely used in rapid prototyping, 3D printing and computer aided designing works. It is easy and simple to output but still some information is lost during conversion to this format. STL format is used for data conversion and data interchange between CAD/CAM systems. In this study the output of the 3D model generated in In-Vesalius can be saved in various formats, but it is saved in ‘.stl’ format because it can be used directly with CAD software.



*Figure 8: Final 3D reconstructed foot*

For this project focus is laid on smaller bones which consists of 1<sup>st</sup> cuneiform, metatarsus and phalanges including proximal and distal phalanges as shown in Fig.9. The required portion of bone is isolated with the help of **Geomagics** CAD software.



*Figure 9: Isolated bone from 3D foot as shown in fig.8 using Geomagics*

### **3.3 DESIGNING OF UNIT LIBRARY STRUCTURE OF SCAFFOLD**

#### **3.3.1 Solidworks**

Solidworks is a computer aided designing (CAD) software which can be used to create new designs, models and structures. It offers designing from scratch and we can create both 3D and 2D

designing in it. Modification of existing designs is possible and various parameters like dimensions, volume, surface area etc. can be calculated. Different parts can be assembled together to make a big functional design. Boolean operations can be used to add, combine and subtract different parts from each other. Multiple views are possible for better and effective design.

### **3.3.2 Criteria's for designing**

Geometric designing of model may include various complex structures and some designs may not be proper for tissue engineering purpose. So it is necessary to formulate some criteria's in order to make a better design. Few criteria's are decided in work by Nattapon Chantarapanich et al. [4]

**Criteria A:** Feasibility of the AM (Additive Manufacturing) technique based production machine.

For example while using various laser based AM techniques like selective laser melting (SLM), selecting laser sintering(SLS) for fabricating porous tissue engineering materials, especially metallic scaffold, the main limitations that concerned were laser spot size and particle size. As a result, the geometric details should be larger than the described limitation of the RP (Rapid Prototyping). This means the first important thing to be kept in consideration before making a design is the manufacturing machine or the rapid prototyping machine.

In the work presented here the rapid prototyping 3D printing machine has the nozzle diameter of 0.2 mm so a structure with minimum dimension of 0.2mm can be made.

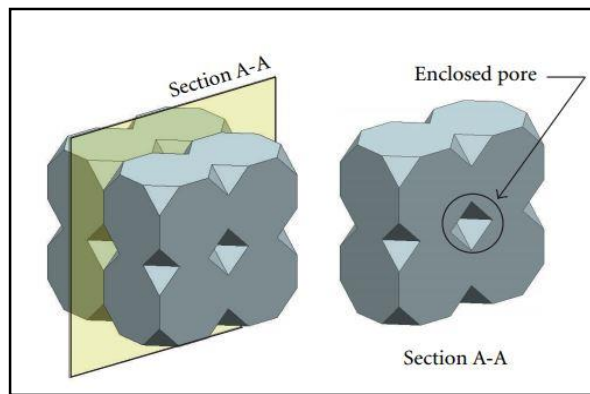
**Criteria B:** Design combinability

Single unit design is combined with other unit design to form a complex matrix structure of scaffold. It is combined along all the axes (x-axis, y-axis and z-axis) hence it should be symmetrical in all the directions. There should be sufficient contact surface between two designs. If the contact

surface of a design is not compatible with the contact surface design of other design then high stress levels may occur at the junctions between them which may ultimately lead to failure of the scaffold.

**Criteria C:** No pores enclosed during the assembly

A certain pore size is required by the cell for proliferation and distribution of nutrients as well as removal of the waste products. Thus it is necessary criteria for a scaffold to be porous. Sometimes due to geometric defect some pores may be blocked, enclosed during assembly. This leads to a problem of deforming a scaffold, the space enclosed within the unit designs is wasted. The following Fig.10 shows a demonstration of enclosed pore.



*Figure 10: Enclosed pores during designing*

### 3.3.3 Porosity of scaffold:

The porosity can be determined by the relationship between the volume of a scaffold material and the volume of apparent scaffold i.e. the virtual bounding box in which the scaffold is designed [4].

The mathematical expression relating to porosity calculation is given by the following equation:

$$\emptyset = 1 - \frac{\text{Volume of scaffold material}}{\text{Volume of apparent scaffold}} \dots\dots\dots (A)$$

Where  $\emptyset$  = porosity

The value of  $\emptyset$  ranges from '0' to '1', the nearly 0 value indicates that the scaffold is dense while the nearly 1 value indicates that the scaffold is porous.

Structurally and mechanically the high porosity scaffold have lower strength when compared with the closed library structure of same design. Because the basic requirement is transportation of fluids, nutrients and waste products as well as proliferation of cells itself, the porosity cannot be eliminated to acquire strength in a design. The higher porosity scaffold may not withstand the loading conditions and may fail [4].

### **3.3.4 Geometric mismatch analysis for merging two different unit structures:**

Many organs have more than one mechanical properties, hence there is requirement of more than one design of unit structure which should be combined with other to achieve better result from the scaffold. The analysis of geometric mismatch was done using two different unit structures (CAD models). Low geometric mismatch refers to large common interface area between the two designs where as high geometric mismatch refers to small common interface at junction of two models.[4] The common interfaces can be measured as intersection index in percentage using equation as described below:

$$\text{Intersection Index (\%)} = \frac{(\text{Contact Area library A}) \cap (\text{contact Area library B})}{\text{Possible maximum contact area}} \times 100 \dots\dots\dots \text{(B)}$$

The larger Intersection Index indicates the better combinability with other design. It is a very important analysis while merging of two or more designs is to be done.

### **3.4 Designs made in Solidworks**

Various sketches, planes and different features of Solidworks are used to create new designs. These designs follow all the criteria as suggested above in 3.3.2. These designs are made in  $3 \times 3 \times 3 \text{ mm}^3$  volume bounding box. All the designs are symmetrical.

To make a new design a new file is created > plane is selected > sketch designed > various features like extrude, extrude cut, swept base, revolve, linear pattern, new planes etc. are used and new designs are created.

As shown in Fig.11 and Fig.12 the designs D1, D2, D3, D4, D5 and D6 are created free form and then D7 is the modified version of D1, D8 is modified version of D4, D9 is modified version of D5 and D10 is modified version of D6. These designs are modified so as to increase the intersection index between different designs.




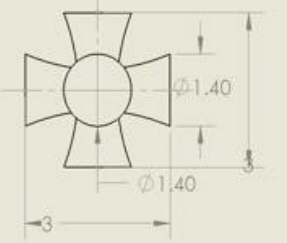
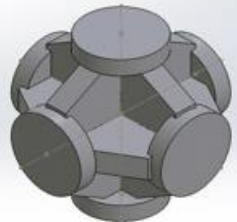
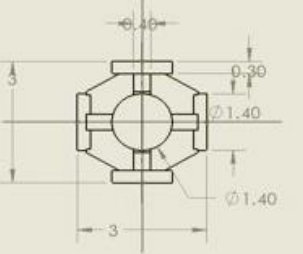

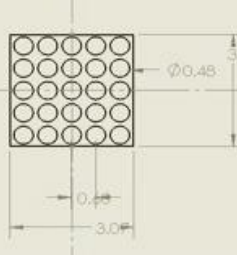
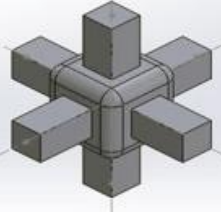
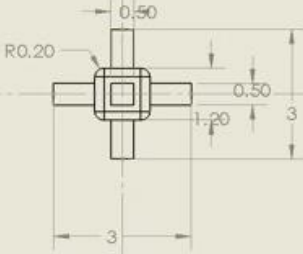
DESIGN	DIMENSIONS (In mm)	Volume (Cubic mm)
D1 		6.05
D2 		6.53
D3 		8
D4 		5.81
D5 		2.97

Figure 11: Designs D1, D2, D3, D4 and D6 in Solidworks



DESIGN	DIMENSIONS (In mm)	Volume (Cubic mm)
D6		3.75
D7		7.17
D8		7.13
D9		4.51
D10		4.79

Figure 12: Designs D6, D7, D8, D9 and D10 in Solidworks

### **3.5 FINITE ELEMENT ANALYSIS IN ANSYS WORKBENCH**

FEA or Finite Element Analysis is method of analysis of physical and behavioral properties of models and designs using numerical calculations and computational simulations. In this process the element is divides into several smaller units, calculations are done for each of these smaller units and collectively the data is processed to give an output.

#### **3.5.1 ANSYS WORKBENCH**

ANSYS Workbench is an analysis software which is used to carryout Finite element analysis and simulations for mechanical designs. We can create virtual environment according to our need, a replica of actual conditions can be created for testing purposes. Simulating our designs and calculations can be done to estimate the flaws in structures. It is a very cost affective and resource saving solution.

#### **3.5.2 Procedure to calculate effective modulus of all the designs using FEA in ANSYS Workbench**

Several steps are involved to obtain solution of FEA in ANSYS as follows

##### **(a) Defining a Material**

The material which is to be used needs to be defined in the software. Here 4 different materials were used as shown in following Table.1

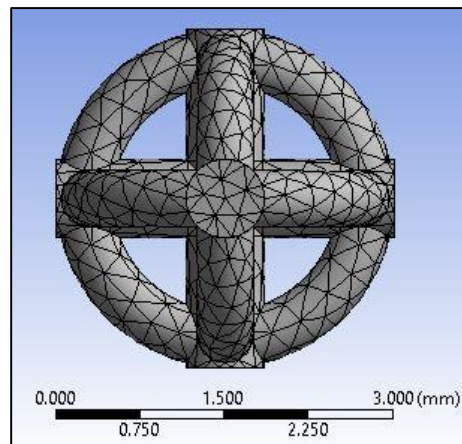
**Table 1: Materials and their mechanical properties for using them in ANSYS [1]**

No	Material	Young's Modulus ( GPa )	Poisson Ratio
1	HA	2	0.3
2	PLLA	2.7	0.3
3	PLGA	4.1	0.3
4	Mat-A	17	0.3

In this study the first 3 biomaterials that are Hydroxyapatite (HA), PLLA, PLGA [1] and a fourth material Mat-A with young's modulus 17 GPa is assumed so that the properties for cortical bones can be analyzed. These materials are defined as linear isotropic and are assigned Poisson ratio of 0.3.

**(b) Importing Model and setting up analysis**

Static structural option in ANSYS Workbench is selected. Using import geometry the design is imported in the modeler. Predefined materials are selected and further part is meshing in which default meshing is selected for the design as shown in Fig.13.



**Figure 13: Meshing in ANSYS**

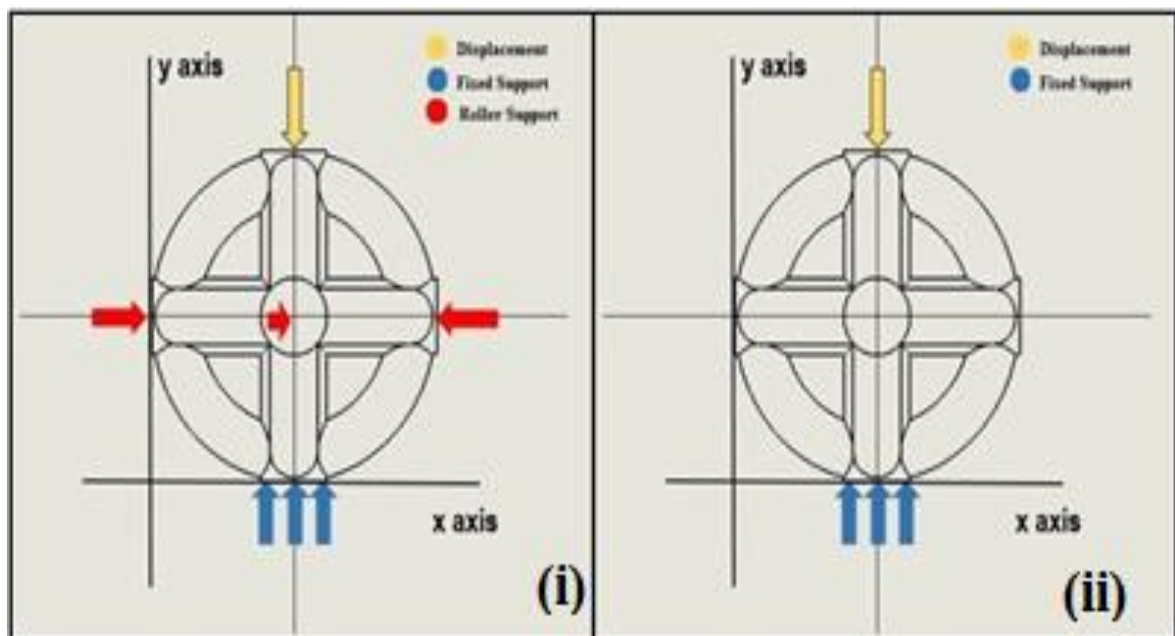
For the analytical setup the model is displaced in y direction while keeping the other opposite end fixed. Now there are two cases:

**i. Confined**

This case as shown in Fig.14 included a fixed support at the opposite end of displacement and roller supports on the remaining sides. This restricted a bulging effect during displacement. It illustrated the properties of scaffold as it may act while placed within a continuum in a global scaffold.

**ii. Unconfined**

This case as shown in Fig.14 didn't include any roller support but only one fixed support. It represents the deformation characteristics of the design without influence of adjacent cells.



*Figure 14: Displacement and supports in (i) Confined case (ii) Unconfined case*

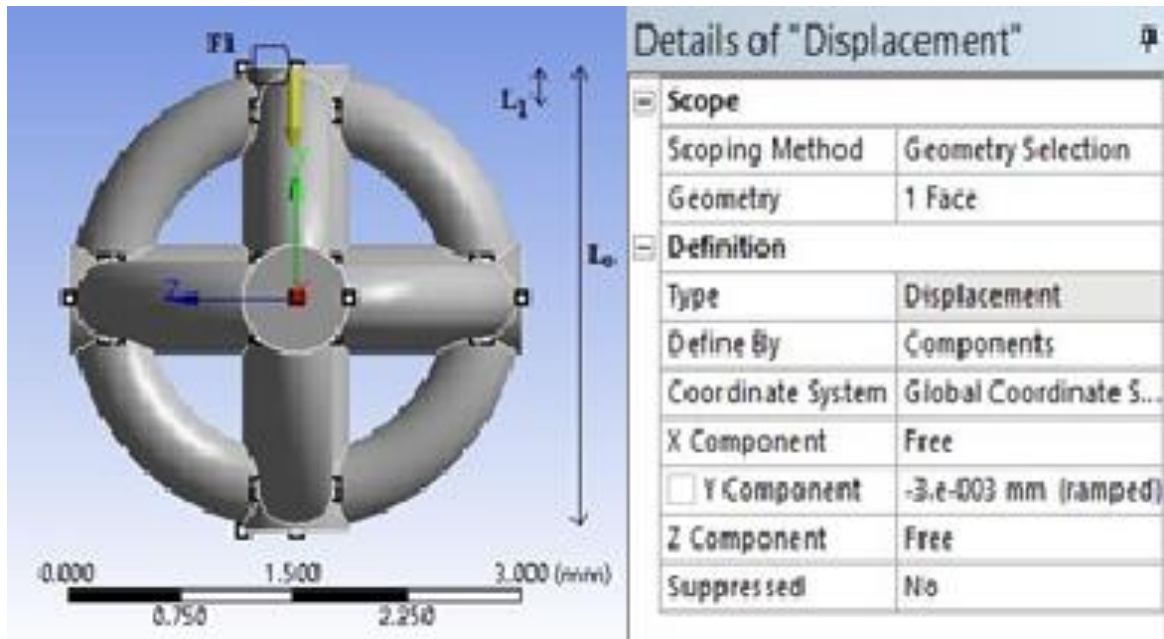


Figure 15: Displacement of the design for calculating Effective modulus

Face  $F_1$  with length  $L_0 = 3\text{mm}$  is displaced in y direction downwards such that the displacement is  $L_1 = 0.001L_0$  which is equivalent to strain  $\epsilon = 0.1\%$  as shown in Fig.15. The boundary condition is intended to obtain a uniform displacement field throughout the design in only y direction. So the effective modulus  $E_y$  is calculated. [1] The effective modulus can be calculated by formula as given below:

$$E_y = \frac{\sigma_y}{\epsilon_y} = \frac{R_y/A_y}{L_1/L_0} = \frac{R_y}{0.001 * A_y} \dots\dots\dots (C)$$

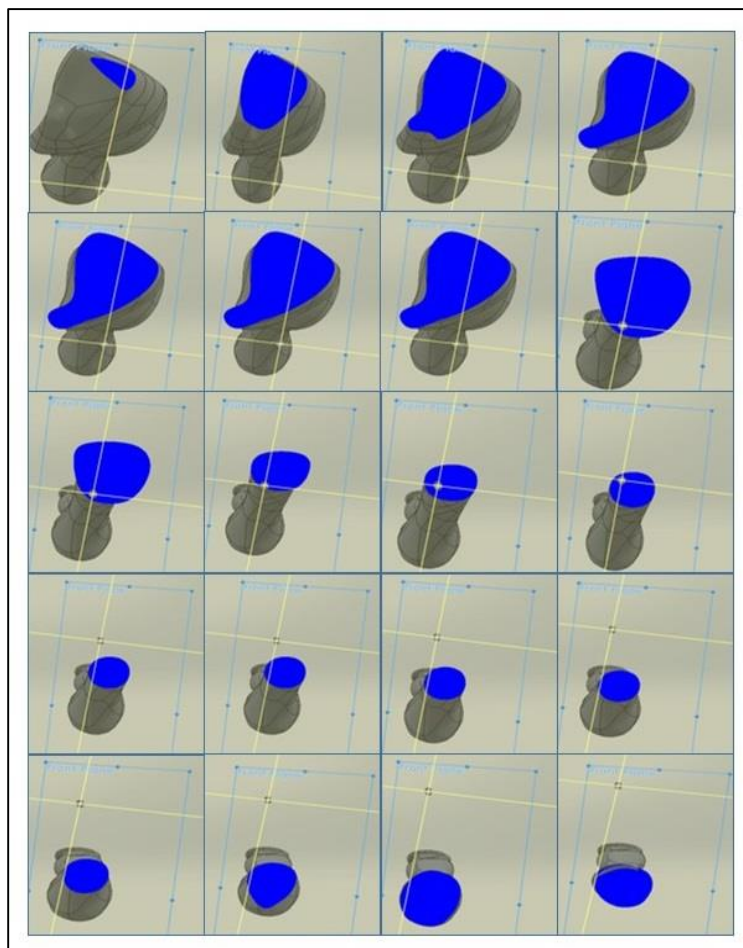
Where  $A_y$  is the area of cross-section on the face  $F_1$  and  $R_y$  is the reaction force at the surface due to displacement in y direction,  $L_0$  is the original length i.e. 3mm and  $L_1$  is the change in length after displacement [ $L_0 - (0.001 * L_0)$ ]. Since the unit cell is symmetric in design in all the x, y and z directions, we have Effective modulus  $E_{\text{Effective}} = E_x = E_y = E_z$ . [1]

### 3.6 SHAPING THE UNIT LIBRARY STRUCTURE IN BONE SCAFFOLD

This process involves the Boolean operations in Solidworks to combine the bone model and the bulk model of unit cell libraries. The bulk structure of unit cell library is superimposed on the recreated bone and combined together using common feature in Solidworks.

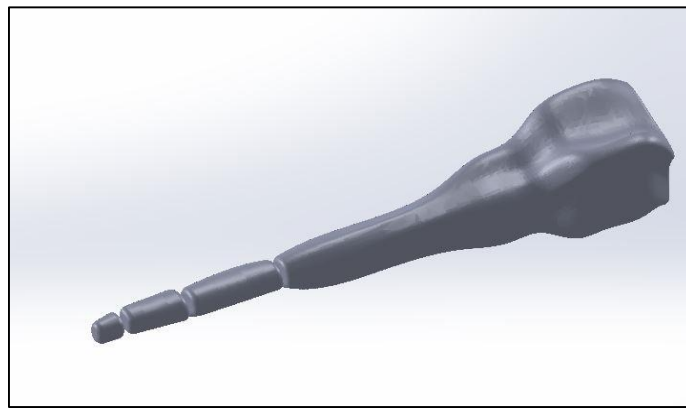
#### 3.6.1 Recreation of the bone part in Solidworks

The isolated bone part in Geomagics has to be recreated so that Boolean operations can be performed in Solidworks. This is done by dividing the bone at equal instances and taking cross-sectional images of the bone in solid works as shown in the Fig.16



*Figure 16: Images showing the cross-sectional planar images of 3D Bone*

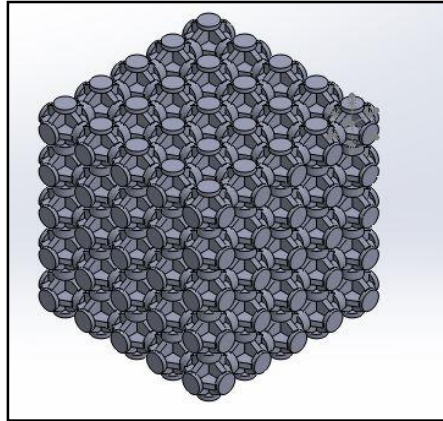
Following the instances, 20 planes were created in solid words and these cross-sectional images were replicated in the form of sketches. Using the lofted base feature in solidworks all of them were connected and finally a bone was recreated as shown in Fig.17. By this method it is not possible to completely replicate the real bone but a similar bone can be obtained which can be used to perform Boolean operations in solidworks.



*Figure 17: Recreated bone in Solidworks*

### **3.6.2 Boolean operations for shaping the scaffold**

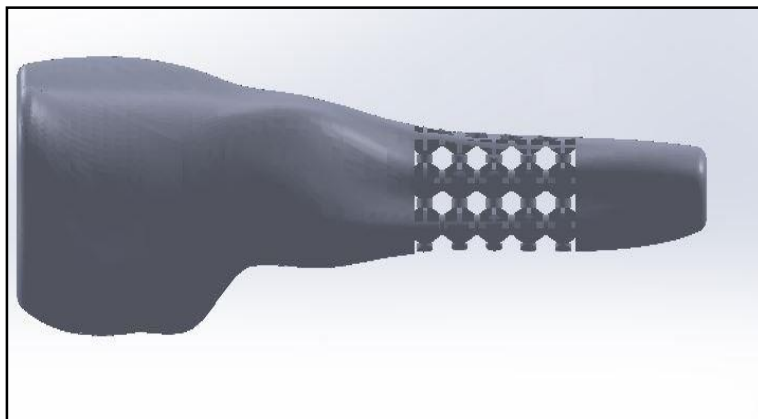
A bulk scaffold model is created in solidworks as shown in Fig.18 using linear pattern. This bulk model is then super-imposed on the bone structure recreated in solidworks and positioned perfectly with matching to the geometry for both objects (bulk scaffold and bone structure). Boolean operation is performed using only the common part and the final structure is saved as a '.stl' file.



*Figure 18: Bulk Structure of D3 unit library design*

### **3.7 FUSED DEPOSITION MODELLING**

FDM technique to print 3D objects was developed in 1989 and it was commercialized first in 1990. It is the second most widely used method for rapid prototyping applications after stereolithography. This rapid prototyping method comprises of computer generated patterns, chemical bonding of polymers, computer numerical mechanism and an extrusion based hardware system to generate 3D objects of the CAD models. This process works layer by layer deposition of thermoplastics in a molten state through a miniature nozzle. The computer generates the raster pattern for the CAD model which is to be printed and then the thermoplastic is heated and delivered on a platform. The model to be printed is shown in Fig.19



**Figure 19: Final demonstration model for 3D Printing**



**CHAPTER 4**

***RESULTS AND DISCUSSION***

#### 4.1 POROSITY

In order to determine the porosity of designs the formula given in **equation (A)** was used.

The porosity result is tabulated in Table.2

*Table 2 Result showing porosity of unit scaffold structure*

<b>Design</b>	<b>Volume of unit scaffold structure mm<sup>3</sup></b>	<b>Volume Apparent scaffold mm<sup>3</sup></b>	<b>(<math>\emptyset</math>) %</b>	<b>Result</b>
D1	6.05	27	77.59	porous
D2	6.53	27	75.81	porous
D3	8	27	70.37	porous
D4	5.81	27	78.48	porous
D5	2.97	27	89.00	porous
D6	3.75	27	86.11	porous
D7(1MODIFIED)	7.17	27	73.44	porous
D8(4MODIFIED)	7.13	27	73.59	porous
D9(5MODIFIED)	4.51	27	83.29	porous
D10(6MODIFIED)	4.79	27	82.25	porous

From biological point of view a desirable scaffold structure should have porosity between 55-70%. Here we observe that all the designs have porosity higher than the standard value and hence it is concluded that all the designs are porous and can be used for scaffold designing.

## 4.2 EFFECTIVE MODULUS OF THE DESIGNS

Effective modulus gives us an idea about the stiffness of the design representing the mechanical strength of the design.

### (i) Confined Case

The calculated reaction forces for confined case are shown in the following Table.3

**Table 3: Reaction force and cross-sectional area for different designs and material in confined conditions**

Design	Hydroxyapatite N	PLLA N	PLGA N	Mat-A N	Cross-sectional area mm <sup>2</sup>
D1	1.3395	1.808	2.7461	11.386	0.38
D2	1.6891	2.2804	3.4628	14.358	1.54
D3	2.3564	3.1811	4.8306	20.029	1.54
D4	1.5417	2.0812	3.1609	13.104	4.7
D5	0.6606	0.8918	1.3543	5.6154	0.25
D6	1.0665	1.4398	2.1863	9.0653	0.42
D7	2.0225	2.7304	4.1462	17.192	1.54
D8	1.7097	2.308	3.5048	14.532	1.54
D9	0.718	0.9693	1.4719	6.1032	1.54
D10	1.1519	1.5551	2.3615	9.7915	1.54

Reaction force values were obtained from ANSYS analysis for all the designs using all the four materials and are shown in columns 2, 3, 4 and 5. All the reaction forces are expressed in Newton.

The cross-sectional area shows the area of contact of the particular design. These values were

substituted in equation (C) to calculate Effective modulus for each combination of material and design. The calculated effective modulus are shown in the following Table.4

**Table 4: Effective modulus of designs with different materials in confined conditions**

<b>Design</b>	<b>Hydroxyapatite GPa</b>	<b>PLLA GPa</b>	<b>PLGA GPa</b>	<b>Mat-A GPa</b>
D1	3.525	4.757895	7.226579	29.96316
D2	1.096818182	1.480779	2.248571	9.323377
D3	1.53012987	2.065649	3.136753	13.00584
D4	0.328021277	0.442809	0.672532	2.788085
D5	2.6424	3.5672	5.4172	22.4616
D6	2.539285714	3.428095	5.205476	21.58405
D7	1.313311688	1.772987	2.692338	11.16364
D8	1.110194805	1.498701	2.275844	9.436364
D9	0.466233766	0.629416	0.955779	3.963117
D10	0.747987013	1.009805	1.533442	6.358117

Young's modulus for cancellous bone is 0.3 GPa to 2 GPa, we observed from Table.4 that when:

- a. HA is used as material - Designs D2, D3, D7 and D8 are promising
- b. PLLA is used as material - Designs D2, D7, D8 and D10 are promising
- c. PLGA is used as material – Designs D4, D9 and D10 are promising

**(ii) Unconfined Case**

The calculated reaction forces for unconfined case are shown in the Table.5

**Table 5: Reaction force and cross-sectional area for different designs and material in unconfined conditions**

<b>Design</b>	<b>Hydroxyapatite N</b>	<b>PLLA N</b>	<b>PLGA N</b>	<b>Mat A N</b>	<b>Cross-sectional area mm<sup>2</sup></b>
D1	1.2642	1.7066	2.5916	10.746	0.38
D2	1.6582	2.2386	3.3994	14.095	1.54
D3	2.2448	3.0305	4.6019	19.081	1.54
D4	1.4581	1.9684	2.9891	12.394	4.7
D5	0.6579	0.8882	1.3488	5.5926	0.25
D6	1.0545	1.4236	2.1617	8.9631	0.42
D7	1.7986	2.4281	3.6872	15.288	1.54
D8	1.606	2.1686	3.293	13.654	1.54
D9	0.7145	0.9646	1.4648	6.0738	1.54
D10	1.1368	1.5347	2.3305	9.663	1.54

Reaction force values were obtained from ANSYS analysis for all the designs using all the four materials and are shown in columns 2, 3, 4 and 5. All the reaction forces are expressed in Newton. The cross-sectional area shows the area of contact of the particular design. These values were substituted in equation (C) to calculate Effective modulus for each combination of material and design. The calculated effective modulus are shown in the following Table.6

**Table 6: Effective modulus of designs with different materials in unconfined conditions**

<b>Design</b>	<b>Hydroxyapatite GPa</b>	<b>PLLA GPa</b>	<b>PLGA GPa</b>	<b>Mat-A GPa</b>
D1	3.326842105	4.491053	6.82	28.27895
D2	1.076753247	1.453636	2.207403	9.152597
D3	1.457662338	1.967857	2.988247	12.39026
D4	0.310234043	0.418809	0.635979	2.637021
D5	2.6316	3.5528	5.3952	22.3704
D6	2.510714286	3.389524	5.146905	21.34071
D7	1.167922078	1.576688	2.394286	9.927273
D8	1.042857143	1.408182	2.138312	8.866234
D9	0.463961039	0.626364	0.951169	3.944026
D10	0.738181818	0.996558	1.513312	6.274675

Young's modulus for cancellous bone is 0.3 GPa to 2 GPa, we observed from Table.6 that when:

- a. HA is used as material - Designs D2, D3, D7 and D8 are promising
- b. PLLA is used as material - Designs D2, D7, D8 and D10 are promising
- c. PLGA is used as material – Designs D4, D9 and D10 are promising

From the results in Table.4 and Table.6 it was observed that a material with 17 GPa young's modulus didn't show acceptable results for cortical bone having young's modulus 13-20 GPa.

### 4.3 INTERSECTION INDEX:

Geometric mismatch can be a very big error for manufacturing of scaffold. Bone being a non-uniform tissue, it has different densities. So in order to replicate its properties we might need to use a combination of two or more unit structure designs depending on their mechanical strength.

**Table 7: Intersection Index for all designs**

Design	Design	D1	D2	D3	D4	D5	D6	D7	D8	D9	D10
	Cross-sectional Area	0.38	1.54	1.54	4.7	0.25	0.42	1.54	1.54	1.54	1.54
D1	0.38	<u>100</u>	<u>100</u>	25	8	66	90	25	25	25	25
D2	1.54	25	<u>100</u>	<u>100</u>	67	16	27	<u>100</u>	<u>100</u>	<u>100</u>	<u>100</u>
D3	1.54	25	<u>100</u>	<u>100</u>	67	16	27	<u>100</u>	<u>100</u>	<u>100</u>	<u>100</u>
D4	4.7	8	67	67	<u>100</u>	5	9	67	67	67	67
D5	0.25	66	16	16	5	<u>100</u>	60	16	16	16	16
D6	0.42	<u>90</u>	27	27	9	60	<u>100</u>	27	27	27	27
D7	1.54	25	<u>100</u>	<u>100</u>	67	16	27	<u>100</u>	<u>100</u>	<u>100</u>	<u>100</u>
D8	1.54	25	<u>100</u>	<u>100</u>	67	16	27	<u>100</u>	<u>100</u>	<u>100</u>	<u>100</u>
D9	1.54	25	<u>100</u>	<u>100</u>	67	16	27	<u>100</u>	<u>100</u>	<u>100</u>	<u>100</u>
D10	1.54	25	<u>100</u>	<u>100</u>	67	16	27	<u>100</u>	<u>100</u>	<u>100</u>	<u>100</u>

From Table.7 we concluded that all the designs with 100% intersection index can be used with each other without consent of geometric mismatch. Moreover larger area of contact between the surfaces of two adjacent structures enables better stress distribution throughout that region.

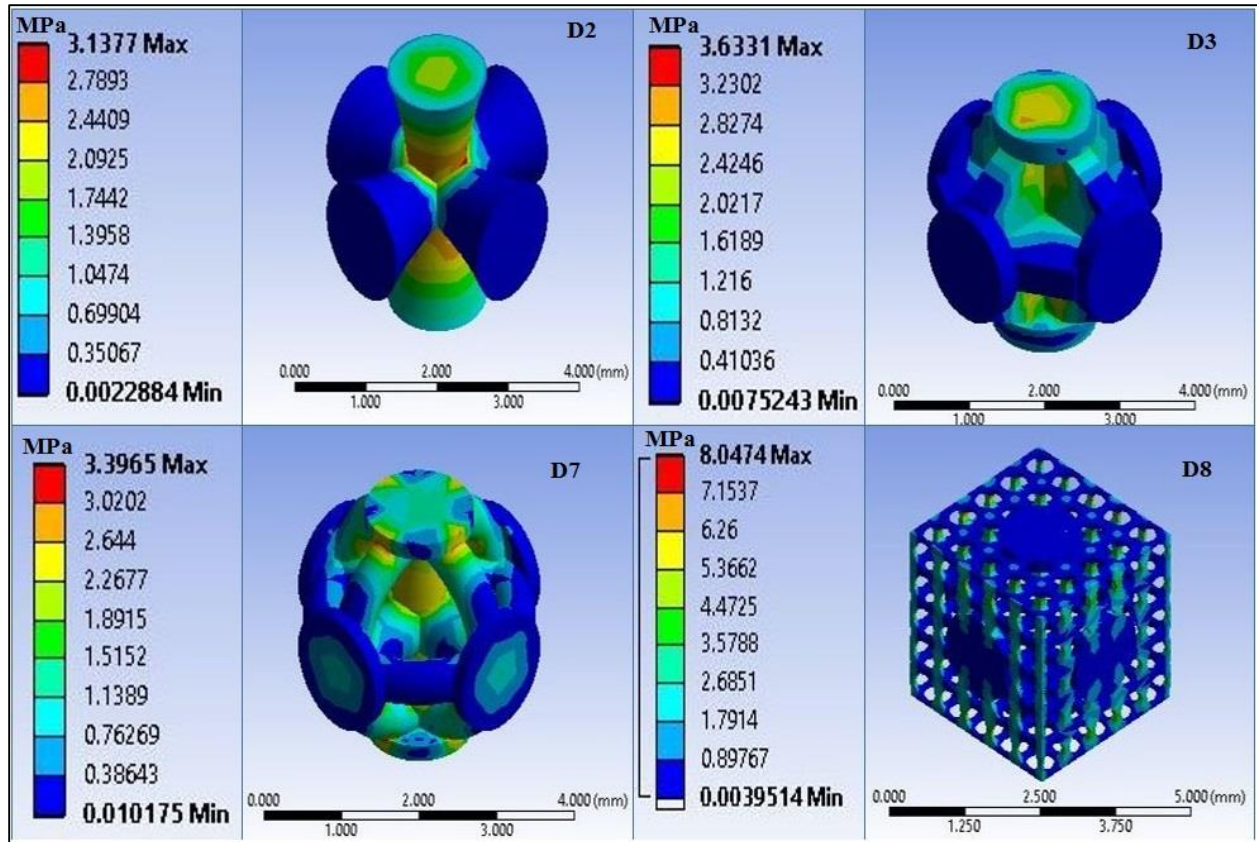
#### 4.4 EQUIVALENT VON MISES STRESS DISTRIBUTION IN DESIGNS:

Hydroxyapatite was considered as a material and all designs were treated with displacement equal to  $0.001*(L_0)$  mm in ANSYS workbench and Equivalent Von Mises stress distribution results were obtained as shown in Table.8

*Table 8: Equivalent Von Mises Stress distribution in all designs.*

<b>Designs</b>	<b>Maximum Equivalent Stress MPa</b>	<b>Minimum Equivalent Stress MPa</b>
<b>D1</b>	6.6124	0.0071
<b>D2</b>	3.1377	0.0022
<b>D3</b>	3.6331	0.0075
<b>D4</b>	5.6885	0.0087
<b>D5</b>	2.8514	0.0003
<b>D6</b>	4.2161	0.0028
<b>D7</b>	3.3965	0.0102
<b>D8</b>	8.0474	0.0039
<b>D9</b>	3.0457	0.0001
<b>D10</b>	4.5780	0.0024





*Figure 20: Equivalent Von Mises Stress distribution D2, D3, D7 and D8*

As observed in Fig.20 in design D2 maximum stress is concentrated towards the center of the design, this is because of the huge edges and comparatively smaller joints towards origin. In D3 the stress is mainly distributed across the displacement axis while it is nearly zero in the remaining sides. In D7 the displacement axis contains huge stress amounts and also the remaining sides contain good amount of stress. In D8 the walls are quite thin and stress is experienced on most of the walls at displacement axis but the origin experiences the maximum stress amongst the given design.

**CHAPTER 5**

***CONCLUSION***

## **CONCLUSION**

The study undertaken in this thesis work presents an application of CATE approach for biomimetic modelling and design of bone –tissue engineered scaffold. In this study the creation of 10 unit structure of libraries for bone scaffolds was demonstrated, that can be used in assembly of a complex structure. These structures are well characterized microstructures that allow scientists to manufacture a superior scaffold with good mechanical properties of localized regions while maintaining incorporation between the adjacent microstructures. As observed in the results the material volume and design of structures were found to affect the mechanical properties and vary accordingly. Due to demands enacted for tissue ingrowth, solid materials will not allow adequate tissue ingrowth and perfusion of fluids and thus porous materials are required which may support such demands. The study demonstrated that the selection of designs D2, D3, D7 are the most suitable designs for cancellous bone scaffolds. Also it was observed that these designs were not suitable for cortical bone scaffold applications because the results obtained did not satisfy the mechanical properties as required by the cortical bone. Materials with higher young modulus may be required for these designs to be used as unit library structure of scaffold for cortical bone.

# ***FUTURE PROSPECTS***

**The future prospects include**

- Research on new biomaterials that can mimic cortical bone's mechanical properties.
- Designing of new structures which can be used for making cortical bone scaffold.
- Working on better designs with lesser resolutions and smaller structures
- Manufacturing of practical scaffold structure and analysis of all supportive property by in-vitro cell culture study
- In vivo study by implanting the artificially created bone in the patient body

# ***REFERENCES***

- [1] W. Sun, B. Starly, A. Darling, and C. Gomez, "Computer-aided tissue engineering: application to biomimetic modelling and design of tissue scaffolds," *Biotechnology and Applied Biochemistry*, vol. 39, pp. 49-58, 2004.
- [2] B. Bucklen, W. Wettergreen, E. Yuksel, and M. Liebschner, "Bone-derived CAD library for assembly of scaffolds in computer-aided tissue engineering," *Virtual and Physical Prototyping*, vol. 3, pp. 13-23, 2008.
- [3] S. Cai and J. Xi, "A control approach for pore size distribution in the bone scaffold based on the hexahedral mesh refinement," *Computer-Aided Design*, vol. 40, pp. 1040-1050, 2008.
- [4] N. Chantarapanich, P. Puttawibul, S. Sucharitpwatskul, P. Jeamwatthanachai, S. Inglam, and K. Sitthiseripratip, "Scaffold library for tissue engineering: a geometric evaluation," *Computational and mathematical methods in medicine*, vol. 2012, 2012.
- [5] M. Wettergreen, B. Bucklen, B. Starly, E. Yuksel, W. Sun, and M. Liebschner, "Creation of a unit block library of architectures for use in assembled scaffold engineering," *Computer-Aided Design*, vol. 37, pp. 1141-1149, 2005.
- [6] K. Iwami and N. Umeda, *Rapid Prototyping in Biomedical Engineering*: INTECH Open Access Publisher, 2011.
- [7] S. A. Skoog, P. L. Goering, and R. J. Narayan, "Stereolithography in tissue engineering," *Journal of Materials Science: Materials in Medicine*, vol. 25, pp. 845-856, 2014.
- [8] D. W. Hutmacher, "Scaffolds in tissue engineering bone and cartilage," *Biomaterials*, vol. 21, pp. 2529-2543, 2000.
- [9] S. Bose, S. Vahabzadeh, and A. Bandyopadhyay, "Bone tissue engineering using 3D printing," *Materials Today*, vol. 16, pp. 496-504, 2013.
- [10] S. Giannitelli, D. Accoto, M. Trombetta, and A. Rainer, "Current trends in the design of scaffolds for computer-aided tissue engineering," *Acta biomaterialia*, vol. 10, pp. 580-594, 2014.
- [11] L. Podshivalov, C. M. Gomes, A. Zocca, J. Guenster, P. Bar-Yoseph, and A. Fischer, "Design, analysis and additive manufacturing of porous structures for biocompatible micro-scale scaffolds," *Procedia CIRP*, vol. 5, pp. 247-252, 2013.
- [12] C. Weinand, I. Pomerantseva, C. M. Neville, R. Gupta, E. Weinberg, I. Madisch, *et al.*, "Hydrogel- $\beta$ -TCP scaffolds and stem cells for tissue engineering bone," *Bone*, vol. 38, pp. 555-563, 2006.
- [13] K. Leong, C. Cheah, and C. Chua, "Solid freeform fabrication of three-dimensional scaffolds for engineering replacement tissues and organs," *Biomaterials*, vol. 24, pp. 2363-2378, 2003.
- [14] A. Shapi'i, R. Sulaiman, M. K. Hasan, A. Y. M. Kassim, and H. A. Hamid, "Applications of Computer Aided Design (CAD) in Medical Image Technology," *International Journal on Advanced Science, Engineering and Information Technology*, vol. 1, pp. 698-701, 2011.
- [15] P. Quadrani, A. Pasini, M. Mattioli-Belmonte, C. Zannoni, A. Tampieri, E. Landi, *et al.*, "High-resolution 3D scaffold model for engineered tissue fabrication using a rapid prototyping technique," *Medical and Biological Engineering and Computing*, vol. 43, pp. 196-199, 2005.
- [16] R. Landers, A. Pfister, U. Hübner, H. John, R. Schmelzeisen, and R. Mülhaupt, "Fabrication of soft tissue engineering scaffolds by means of rapid prototyping techniques," *Journal of materials science*, vol. 37, pp. 3107-3116, 2002.
- [17] S. H. Masood and K. Alamara, "Development of scaffold building units and assembly for tissue engineering using fused deposition modelling," in *Advanced Materials Research*, 2010, pp. 269-274.
- [18] <http://www.physicscentral.com/explore/action/images/scans-img2.gif>
- [19] <http://fieremans.diffusion-mri.com/phd/PhD89x.png>

- [20] [www.microdicom.com](http://www.microdicom.com)
- [21] <http://svn.softwarepublico.gov.br/trac/invesalius>
- [22] <http://www.osirix-viewer.com/datasets/>